In-wheel Motor Electric Vehicle Based on Fuzzy Neural Network Yaw Stability Optimization Control

Zhigang Zhou, Xinqing Ding, Zhichong Shi, Xiaofei Yin, Xiangming Meng.

Abstract—**To improve the control accuracy of the stability control system of electric vehicles driven by in-wheel motors, the Particle swarm optimisation (PSO) Fuzzy neural network (FNN) in the late convergence of local extreme value and convergence speed and accuracy reduction. The Unscented Kalman filter (UKF) state observer is built to observe the sideslip angle to improve the control accuracy of the vehicle stability control system. An FNN control method is proposed based on improved particle swarm optimisation (IPSO-FNN). The velocity term of the particle in the particle swarm is removed, the position term is optimised, the extreme value of individual particles is extracted randomly, and the position term, personal optimal solution and global optimal solution are calculated. At the same time, the Laplace coefficient is introduced to avoid a locally optimal solution. Finally, the additional yaw moment is calculated by IPSO-FNN, and the optimal torque distribution is carried out with the minimum tire longitudinal force as the optimisation objective. The results show that the overshoot of the sideslip angle is reduced by 27%, and the convergence rate is increased by 2.5%. The problem of local extreme value in the control of the FNN is avoided, and the driving stability of the electric vehicle driven by the in-wheel motor is improved.**

Index Terms—**In-wheel motor, State observation, PSO, Yaw moment, Moment distribution.**

I. Introduction

IN-WHEEL motor is the integration of power, transmission, and braking so that the vehicle hub becomes an independent power unit. It features independent and controllable drive wheel torque, high transmission efficiency, fast response speed, and easy modularisation. These advantages can effectively improve the handling stability, power, economy, and active safety of electricity [1]. Therefore, In-wheel motor drive technology is one of the development directions of advanced automatic driving and has gradually become a research hotspot for experts and scholars [2]. As for the vehicle yaw moment of the vehicle handing stability, it is decisive. At present, many advanced control theories, such as sliding mode control [3], FNN [4-5], and model prediction [6-7], are used to plan the yaw moment of an EV driven by an in-wheel motor. The FNN is widely used among them due to its excellent nonlinear performance, self-learning capability and other advantages. However, FNN has problems such as complex parameter learning, slow convergence speed and easy falling into local extremum, which need improvement [8].

PSO, a swarm-intelligent stochastic optimisation algorithm, has a robust global search ability and is more widely used in the optimisation problems of neural networks and fuzzy control [9-10]. Knapsack problem [11], path planning [12]. However, like most optimisation algorithms, PSO tends to fall into local optimum in the later stage of convergence, and its convergence accuracy and speed would decrease [13]. Therefore, many researchers have successively improved standard particle swarm optimisation from different perspectives to improve the optimisation performance of the particle swarm optimisation algorithms. Literature [14] proposes a random weight particle swarm optimisation algorithm to identify the dynamic parameters, improving the robot's dynamic parameters' identification accuracy; a solution strategy is proposed to solve the p-Hub allocation problem based on the PSO algorithm with different inertia weights. The optimal improved PSO algorithm, cat swarm optimisation (CSO) and harmony search (HS) algorithm are selected to optimise the P-Hub allocation problems. Simulation results verify the effectiveness of the improved PSO algorithm [15].

Literature [16] proposes the velocity term in the standard PSO algorithm is removed, the second-order differential equation is changed into the first-order, and the position term is independently optimised and controlled, which can effectively avoid the problems of decreasing convergence speed and low accuracy in the later stage of PSO; Literature [17] proposes particle inertia factor was added and a PSO algorithm combining inertia weight and learning factor was proposed, which improved the optimisation accuracy and rate of convergence. Literature [18] suggests a single position term optimisation is adopted, and the mean of the individual extreme value of each particle is taken as the personal extreme value of the individual particle enabling the algorithm to adjust the acceleration coefficient automatically.

Manuscript received May 6, 2023; September 18, 2023. This work was supported by the National Natural Science Foundation of China (51805149); and Ningbo Science and Technology Innovation 2025 Major Special Project "Development of Light Electric Vehicle In-wheel Motor and Control System" (2019B10073).

Zhigang Zhou is an associate professor of Henan University of Science and Technology, Luoyang, 471003, China. (corresponding author, phone: +86 15137976859; e-mail: zhigangzhou@haust.edu.cn).

Xinqing Ding is a postgraduate student of Henan University of Science and Technology, Luoyang, 471003, China. (e-mail: m18438114984@163.com).

Zhichong Shi is a postgraduate student of Henan University of Science and Technology, Luoyang, 471003, China. (e-mail: 2950469826@qq.com).

Xiaofei Yin is a postgraduate student of Henan University of Science and Technology, Luoyang, 471003, China. (e-mail: yxfhch@163.com).

Xiangming Meng is a postgraduate student of Henan University of Science and Technology, Luoyang, 471003, China. (e-mail: mxm @ haust.edu.cn).

A modified PSO algorithm is proposed to optimise FNN, which can optimise the standard PSO algorithm. The Laplace coefficient is used to improve the population universality of PSO, and the inertia weight factor and the dynamic learning factor are used to improve the accuracy and convergence rate of the optimisation. By establishing a layered control system for the yaw stability of an electric vehicle driven by an in-wheel motor, the yaw velocity and sideslip angle of the vehicle were taken as the control objectives. The additional yaw moments required for stable driving of the vehicle were calculated, and the distribution of wheel drive torque was optimised. In addition, to improve the control accuracy of control variables, a state observer model of vehicle driving based on UKF is established. It significantly enhances the lateral stability of the electric vehicle driven by the in-wheel motor, avoiding dangerous conditions such as rollovers and skids, and provides reasonable control.

II. Vehicle Dynamic Model

A. Whole Vehicle dynamics model

This paper adopts the model of electric vehicles driven by front-wheel steering and four wheels driven by in-wheel motors, assuming that the car runs smoothly under good road conditions, ignoring the vertical movement, pitch movement, and roll motion [19], and assuming equal front and rear wheel pitches, take the front wheel corner as input. Establish the vehicle dynamics modelling with three degrees of freedom as shown in Figure 1: longitudinal, lateral and yaw.

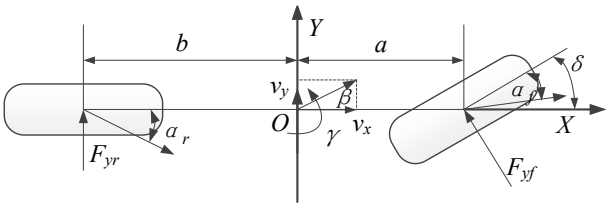

Fig. 1. Three degrees of freedom vehicle model

According to Newton's laws of mechanics, linear equations in the x, y, and z directions can be obtained:

$$\begin{cases} \dot{v}_y = -v_x\gamma + \dfrac{aC_x - bC_y}{mv_x}\gamma + \dfrac{(C_x + C_y)v_x}{mv_x} - \dfrac{C_x}{m}\delta \\ \dot{v}_x = v_y\gamma + a_x \\ \dot{\gamma} = \dfrac{a^2C_x + b^2C_y}{I_z v_x}\gamma + \dfrac{aC_x - bC_y}{I_z}\beta - \dfrac{aC_x}{I_z}\delta \\ \beta = \arctan(\dfrac{v_x}{v_y}) \\ a_y = \dfrac{aC_x - bC_y}{mv_x}\gamma + \dfrac{C_x + C_y}{m}\beta - \dfrac{C_x}{m}\delta \end{cases} \tag{1}$$

In equation *a, b* is the distance from the centre of mass to the anterior and posterior axes; γ is the yaw velocity of the wheel hub motor electric vehicle; a_x is longitudinal acceleration; a_y is the lateral acceleration; C_x, C_y for the longitudinal and lateral stiffness of the tire; β is the sideslip angle of the wheel motor electric vehicle; δ is the front wheel steering angle of the wheel motor electric vehicle.

B. Tire model

For computational ease, a Duogff tire model with fewer parameters is used in this paper to obtain the longitudinal force F_x and the lateral force F_y that the tire needs to withstand;

$$\begin{cases} F_x = \mu F_z C_x \dfrac{\lambda}{1-\lambda} f(L) \\ F_y = \mu F_z C_y \dfrac{\tan\alpha}{1-\lambda} f(L) \end{cases} \tag{2}$$

$$f(L) = \begin{cases} L(2-L), L < 1 \\ 1, \quad L \geq 1 \end{cases} \tag{3}$$

$$L = \frac{(1-\lambda)(1-\varepsilon v_x\sqrt{C_x^2\lambda^2 + C_y^2\tan^2\alpha})}{2\sqrt{C_x^2\lambda^2 + C_y^2\tan^2\alpha}} \tag{4}$$

$$\begin{cases} F_{zfl,zfr} = (\dfrac{1}{2}mg \pm m\dfrac{a_y h}{d})\dfrac{a}{l} - \dfrac{1}{2}\mathrm{ma}_x\dfrac{h}{l} \\ F_{zrl,zrr} = (\dfrac{1}{2}mg \pm m\dfrac{a_y h}{d})\dfrac{b}{l} - \dfrac{1}{2}\mathrm{ma}_x\dfrac{h}{l} \end{cases} \tag{5}$$

In the equation, F_z is the vertical load of the tires of the in-wheel motor electric vehicle; μ is the road adhesion coefficient; λ is the tire slip rate; ε is the speed influence coefficient of the in-wheel motor electric vehicle; α is the side slip angle of the in-wheel motor electric vehicle; h is the height of the vehicle centroid; l is the distance between the front and rear axles of the car, $l = a + b$.

C. Design UKF filter observer

UKF filters vehicle status observations

UKF is a new nonlinear filtering algorithm that uses Unscented Transform to determine sample points to improve the accuracy of mean and covariance in nonlinear states, better represent probability densities, and simplify calculations [20]. According to the UKF flow range shown in Figure 2, continuous iteration and updating are carried out to obtain the optimal vehicle driving state and road surface adhesion coefficient observations.

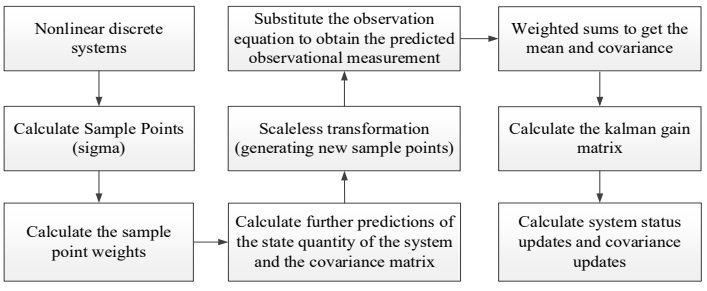

Fig. 2. UKF flow chart

The equation for the state space of a nonlinear system can be expressed in the following form:

$$\begin{cases} x(k+1) = f(x(k)) + w(k) \\ z(k) = h(x(k)) + v(k) \end{cases} \tag{6}$$

$x(k)$ is the state vector of the observing system; $z(k)$ is the observation vector; let h be a metric function; $w(k)$ and $v(k)$ are process noise and measurement noise, respectively.

In this paper, the longitudinal velocity, yaw velocity, and side-slip angle of the car are set as state variables, $\boldsymbol{x} = [v_x, \gamma, \beta]$.

The lateral acceleration is used as the measurement variable, and the front wheel angle and longitudinal acceleration are used as input control variables, Simulink and Carsim were co-simulated, the Carsim simulation speed is set to 80 km/h, and the road adhesion coefficient *is* μ = 0.8. Therefore, the UKF-based sideslip angle observer estimation results are shown in Figure 3. Figure 4 shows the observation error of the sideslip angle. The average estimation error of the UKF observer does not exceed 0.002 rad; the observations are ideal and meet the conditions of use of the vehicle stability control system.

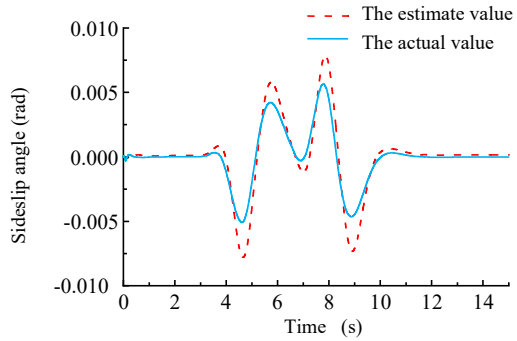

Fig. 3. Observation results of UKF the sideslip angle response

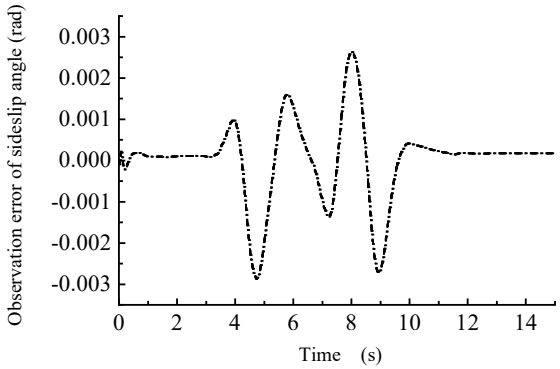

Fig. 4. Observation error of sideslip angle

III. Design of Vehicle Control System

The lateral stability control system of the vehicle is designed using hierarchical control. The upper layer is the motion tracking layer, which takes the difference between the declination angle and the yaw velocity of the ideal sideslip angle and the actual sideslip angle and the yaw angle velocity as inputs, respectively. The additional yaw moment that allows the car to run stable is calculated by the lower layer is the torque optimisation distribution layer, which designs the optimal distribution method for the five tire forces, so that the dynamic performance of the vehicle's drive system is optimised and the driver can stably drive the car according to the driver's wishes. See Fig. 5 for a schematic view of the structure of the control system of an electric vehicle driven by an in-wheel motor.

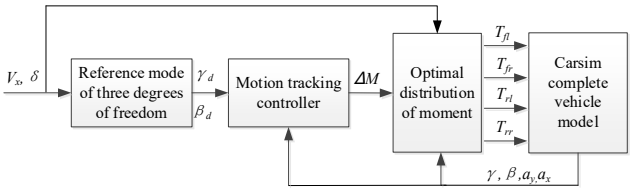

Fig. 5. Structure diagram of vehicle control system

A. Upper-level control

Fuzzy neural networks

To simplify calculations and reduce the complexity of the control system, the FNN controller uses a two-input one-output approach. The FNN in the form of multiple inputs and single outputs is used to calculate the additional yaw moment ΔM of the vehicle, as shown in Figure 6. The FNN is divided into five layers, with the first three being the front and the last two being the judgment part.

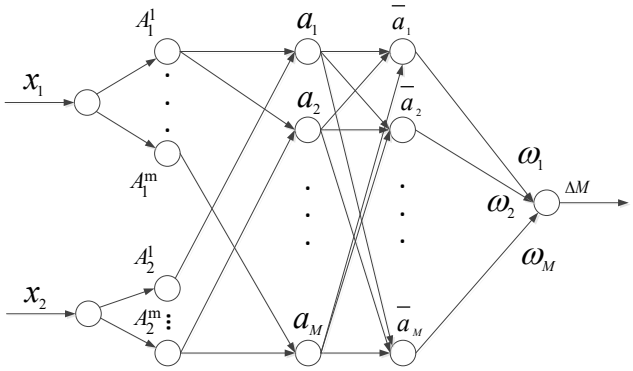

Fig. 6. FNN network structure diagram Input layer, Membership function layer, Rule layer, Normalized layer, Anti-fuzzification layer

The first layer: the input layer, with two input quantities x_1 and x_2, which are the deviation between the actual and theoretical values of the yaw velocity and the sideslip angle $\Delta\gamma$ and $\Delta\beta$; control it within [-1,1] using the hyperbolic tangent function.

$$x_1 = \frac{1 - e^{-\Delta\gamma.\rho 1}}{1 + e^{-\Delta\gamma.\rho 1}} \tag{7}$$

$$x_2 = \frac{1 - e^{-\Delta\beta.\rho 2}}{1 + e^{-\Delta\beta.\rho 2}} \tag{8}$$

Above ρ_1 and ρ_2 are the scale factors.

The second layer: the fuzzy inference layer, sets the fuzzy set of input amounts $\Delta\gamma$ and $\Delta\beta$ and uses the gaussmf function as its membership function type,

$$A_i^j = e^{(\frac{x_i - b_{ij}}{\delta_{ij}})^2}, i = 1,2; j = 1,2,\cdots,5 \tag{9}$$

The third layer: the rule layer, normalizes the nodes of the fuzzy inference layer according to the fuzzy rule and computes their weights, viz.

$$a_M = A_1^m \cdot A_2^k \quad m,k = 1,2,\cdots,5; \quad M = 1,2,\cdots,25 \tag{10}$$

The fourth layer: the conclusion layer, calculates the excitation intensity of the current input to the fuzzy rule $\bar{a}_M$

$$\overline{a}_M = \frac{a_M}{\sum_{n=1}^{25} a_n} \tag{11}$$

The fifth layer: the output layer, outputs clear fuzzy variables and obtains an additional yaw moment *ΔM*.

$$\Delta M = \overline{a}_M \times \omega_M, M = 1,2,\cdots,25 \tag{12}$$

Improved PSO algorithm

The convergence speed of the standard PSO algorithm gradually decreases in the later stage of optimisation, and it is easy to fall into the local extreme, resulting in a poor convergence effect. The standard PSO algorithm determines the direction and distance of the optimal search by the position and speed of each particle. It is continuously updated at each iteration by keeping track of its extreme value and the overall extreme value.

$$\begin{cases} v(t+1) = wv(t) + c_1 r_1 (p_{Beat}(t) - x(t)) + \\ c_2 r_2 (g_{Beat}(t) - x(t)) \\ x(t+1) = x(t) + v(t) \end{cases} \tag{13}$$

The equation: t is the number of iterations; p_{Beat} is an individual extremum; g_{Beat} is the overall extremum; c_1 and c_2 are acceleration coefficients; r_1, r_2 are random numbers.

To improve the optimisation ability of all particles and fully utilize the information contained in all particles, literature [15] simplified the iterative formula of the particle swarm, transforming the second-order optimisation differential equation into a first-order equation, simplifying calculations and improving the efficiency of the algorithm:

$$x(t+1) = wv(t) + c_1 r_1 (p(t) - x(t)) + c_2 r_2 (g_{Beat}(t) - x(t)) \tag{14}$$

There into,

$$p(t) = 1/N \sum_{i=1}^{N} p_{Beat}(i)$$

Due to the strong controllability of the acceleration coefficients c_1 and c_2, which respectively serve as "cognition" and overall "guidance" for individual particles, the early pursuit of excellence has global search ability, with the hope of having a larger c_1 and a smaller c_2. At later stages, it is desirable to have a smaller c_1 and a larger c_2 to improve the convergence rate and accuracy, so c_1 and c_2 are taken as follows:

$$c_1(t) = 1 - \exp(-|F_{avg}(t) - F_{g_{Beat}}(t)|) \tag{15}$$

$$c_2(t) = 1 - c_1(t) \tag{16}$$

Thereinto,

$$F_{\text{avg}}(t) = 1/N \sum_{i=1}^{N} f(x_i(t)), Fg_{Beat}(t) = f(g_{Beat}(t))$$

At the same time, to avoid premature convergence, equation (15) has been improved, taking into account the influence of a single random candidate solution and incorporating the Laplace coefficient. An inertial weight factor for out-of-synchronous transitions and a dynamic learning factor ci(t) are introduced to improve convergence speed and accuracy further. The improved location items are as follows:

$$\begin{aligned} x(t+1) = {} & wx(t) + c_1 r_1 (p_{Beat}(t) - x(t)) + \\ & c_2 r_2 (g_{Beat}(t) - x(t)) + \lambda\xi[p_i(t) - x(t)] \end{aligned} \tag{17}$$

In the equation, $p_i(t)$ is an individual random candidate solution.

The Laplace function is

$$F(x) = \begin{cases} 1/2 \exp(\frac{x-\sigma}{\omega}) & x < \sigma \\ 1 - 1/2 \exp(\frac{\sigma - x}{\omega}) & x \geq \sigma \end{cases} \tag{18}$$

In the equation, σ and ω are the Laplace function's location and scale parameter rates, respectively.

$$\lambda = \begin{cases} \omega \ln(2u) & u < 0.5 \\ -\omega \ln(2-2u) & u \geq 0.5 \end{cases} \tag{19}$$

To reduce the effect of λ, the constraint function ζ is added.

$$\xi = (1 - \frac{t}{t_{\max}})^b \tag{20}$$

The expressions for the inertial weighting factor and the dynamic learning factor are as follows:

$$w(t) = w_{\max} - \frac{w_{\max} - w_{\min}}{t_{\max}} \times t \tag{21}$$

$$\begin{cases} c_1(t) = A - \lambda t \\ c_2(t) = B + \lambda t \end{cases} \tag{22}$$

In the equation: $t_{\max}$ is the maximum number of iterations; $w_{\max}$ is the maximum inertia factor in the optimisation; $w_{\min}$ is the minimum inertia factor in the optimisation; c_1 and c_2 are linear functions of the number of iterations, in addition to A = 2.5 and B = 0.5.

This section simplifies the PSO and calculates the position term by randomly extracting the extreme values of a single particle, together with the individual optimal solution and the overall optimal solution. The inertia weight and learning factor are dynamically adjusted, and the Laplace coefficient is introduced to improve the particle swarm, forming different improved PSO optimisation algorithms.

FNN Optimization based on improved PSO

In an FNN control system, where the first three layers are fuzzy layers with nonlinear parameters, and the last two layers are conclusion layers with linear parameters, Gradient Descent and Least Squares methods are commonly used in optimal control process. But Gradient descent is mainly used to solve unconstrained optimisation problems, while Least squares are slow to converge for strongly nonlinear problems and tend to fall into local extremes.

PSO algorithm is a stochastic optimisation algorithm that simulates the birds' self-organising behavior; In this paper, an improved PSO algorithm is proposed to optimise the FNN by optimally adjusting the weights of the fuzzy rules to improve the convergence speed and accuracy of the system; and the optimisation procedure is shown in Figure 7. Improve the PSO algorithm, simplify the PSO, and randomly extract the extremum of a single particle to share the individual optimal solution and the overall optimal solution. Using the dynamic adjustment method for inertia weight and learning factor, and introducing the Laplacian system for calculating position terms number, improve particle swarm optimization to form different improved PSO optimization algorithms;

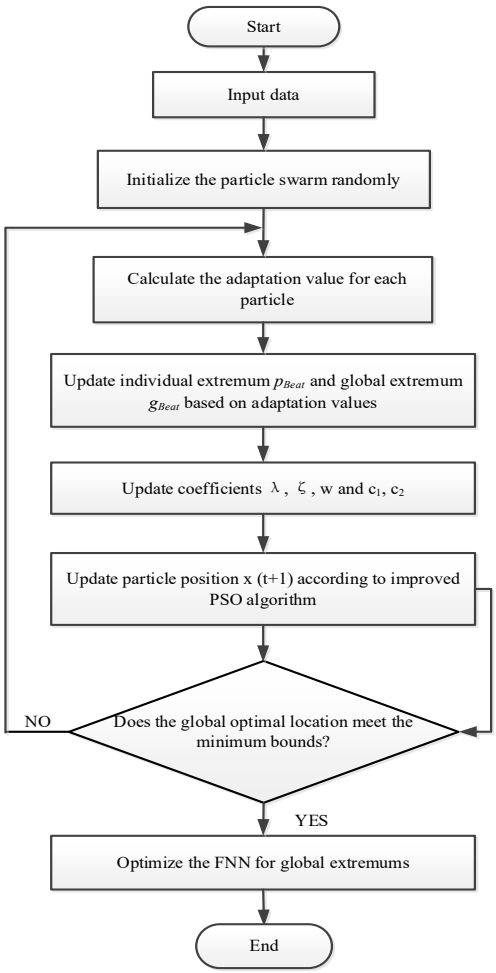

Fig. 7. Improved PSO-FNN process

B. Lower control layer

The lower control layer is the torque optimisation distribution layer, which distributes the additional yaw-moment ΔM calculated by IPSO-FNN to stabilise the vehicle and the longitudinal vehicle demand torque to the drive wheels. Due to the independent and controllable structure of the four-wheel torques of the wheel motor-driven electric vehicle, the control system is an overdrive control system that needs to optimise the distribution of the demand torque to each wheel. Considering the constraints of the tyre attachment ellipse, to obtain the maximum vehicle lateral margin, the objective of the optimisation is to minimise the longitudinal force of each tyre and establish the objective function as follows.

$$\min J = \sum_{i=1}^{4} \frac{F_{xi}^2}{(\mu F_{zi})^2} = u_1^{\ T} W u_1 \tag{23}$$

$$\begin{cases} F_x = F_{fl} + F_{fr} + F_{rl} + F_{rr} \\ M_z = \dfrac{T}{2}(-F_{fl} + F_{fr} - F_{rl} + F_{rr}) \end{cases} \tag{24}$$

Write equation (24) in matrix form:

$$x = E u_1 \tag{25}$$

$$x = [F_x \; M_z]^{\mathrm{T}} \quad u_1 = [F_{fl} \; F_{fr} \; F_{rl} \; F_{rr}]^{\mathrm{T}}$$

$$E = \begin{pmatrix} 1 & 1 & 1 & 1 \\ -\dfrac{d}{2} & \dfrac{d}{2} & -\dfrac{d}{2} & \dfrac{d}{2} \end{pmatrix}$$

Considering the external characteristics of the motor and the longitudinal force of the wheel of a hub motor car subject to the coefficient of adhesion and vertical load, the constraints are:

$$-\frac{T_{i\max}(x)}{r} \le F_i \le \frac{T_{i\max}(x)}{r}$$

$$-\mu F_{zi} \le F_i \le \mu F_{zi}$$

In the equation, M_z is the total demand moment.

Transforming equation (26) into a sequential Least squares problem as $\min \left\| E u_1 - x \right\|_2$

$$W = \mathrm{diag}\left(\frac{1}{(\mu F_{zi})^2} \right)$$

$$\begin{cases} u_1 = \arg\min\limits_{uc \in \Omega} \left\| W_{u_1} u_1 \right\|_2 \\ \Omega = \arg\min \min\limits_{uc^- \le uc \le uc^+} \left\| W_x (E u_c - x) \right\|_2 \end{cases} \tag{26}$$

In the equation, W_{u1}, W_x is the weight matrix.

The introduction of a weighting factor ψ transforms serial Least squares into a weighted least squares problem:

$$u_c = \arg \min_{uc^- \le uc \le uc^+} \left(\left\| W_{u_1} u_c \right\|_2^2 + \psi \left\| W_x (E u_c - x) \right\|_2^2 \right) \tag{27}$$

The actuator distributes the calculated drive torque for each wheel to each drive wheel.

IV. Simulation Analysis

To verify the effectiveness of the improved PSO-optimized FNN control system proposed in this study, a joint simulation of Carsim and Simulink is used. There are some differences in the power transmission system between single-motor and dual-motor drive vehicles and in-wheel motor drive electric vehicles. In Carsim parameter design, the power transmission system is modified to an external model input to the wheels. The whole vehicle parameters are shown in Table I, and the changes in yaw velocity and sideslip angle were compared before and after the optimisation of the FNN, using the double line change condition as an example.

The simulated vehicle speed is 80 km/h, and the road adhesion coefficient μ is 0.8. The simulation results are shown in Figures 8-12, and Figure 8 shows the steering wheel angle. Figure 9 shows the speed change curve under FNN control after PSO optimisation. It can be seen that the optimized speed response curve has less fluctuation and can maintain the vehicle speed well. Figure 10 shows that by optimising the moment distribution, the lateral acceleration is controlled to within 0.4 m/s^2, indicating that the yaw moment control can ensure vehicle motion stability. From the longitudinal vehicle speed in Figure 9 and the lateral acceleration response curve in Figure 10, it can be concluded that vehicles based on control strategies have better stability and tracking ability.

Fig. 11 and Fig. 12 show the response curves of the vehicle under FNN control and improved PSO-optimized FNN control for yaw velocity and sideslip angle with their ideal values, respectively.

As shown in Figure 11, the control differences between the two control methods are minor and both enable γ to follow the ideal value better. Due to the limitation of yaw velocity, the vehicle appears slightly smaller at the ideal corner; but at the rest of time, the yaw velocity γ there is almost no error, perfectly tracking the ideal yaw velocity; Figure 12 shows

that the IPSO-FNN control has 27% less overshoot than the FNN control for the sideslip angle, while the convergence rate increases by 2.5%. When FNN is controlled, the adaptive ability is poor, and the vehicle overshoot increases significantly, the jitter increase is more prominent, compared to FNN, IPSO-FNN self-adaptive has a smaller jitter and better tracking effect of sideslip deflection angle. The vehicle is also in a stable state.

It can be seen that IPSO-FNN can better track the ideal sideslip angle, improve the accuracy of the rate of convergence of the wheeled electric vehicle's lateral stability control system, ensure the vehicle's driving stability, and ensuring driving safety.

TABLE I
VEHICLE PARAMETERS

Name	Value	Name	Value
The mass m /kg	1429	Rotational inertia moment around z-axis I_z /kg(m^2)	1765
Car mass height h /m	0.67	Front and rear axle spacing l /m	2.619
Front-wheel spacing T_f /m	1.565	Tyre rolling radius R /m	0.357
Rear wheel spacing T_r /m	1.565	Front-wheel lateral deflection stiffness C_f /kN(rad)	-40000
Distance from centre of mass to front axle a /m	1.05	Rear wheel lateral deflection stiffness C_r /kN(rad)	-50000
Distance from centre of mass to rear axle b /m	1.569	Gravity acceleration g /m/s^2	9.8

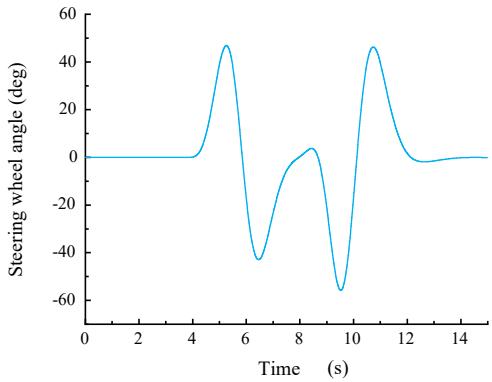

Fig. 8. Steering wheel angle

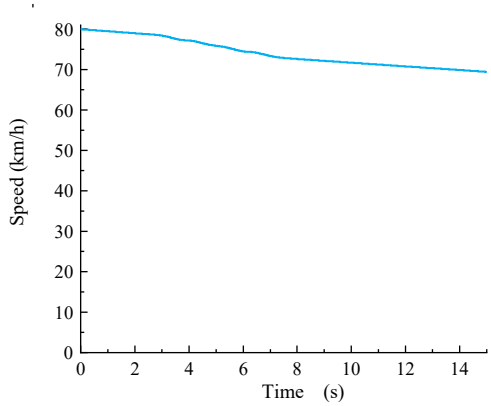

Fig. 9. Longitudinal speed

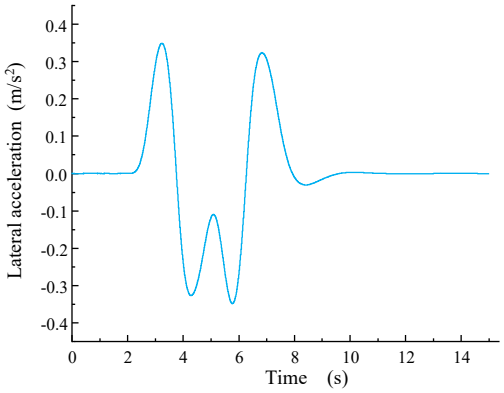

Fig. 10. Lateral acceleration

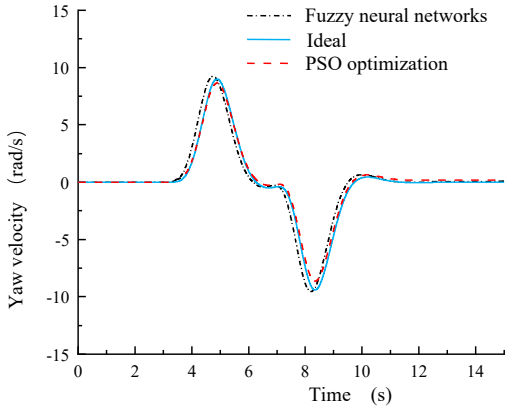

Fig. 11. Yaw velocity response

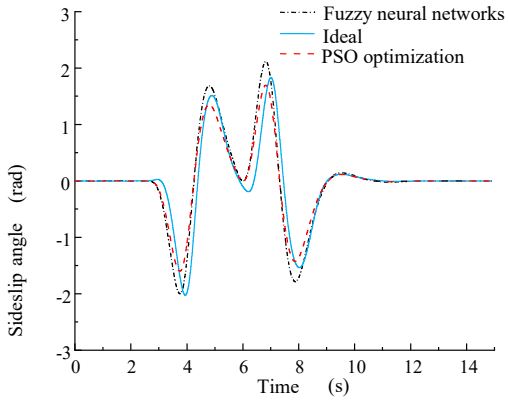

Fig. 12. Sideslip angle response

V. CONCLUSION

A UKF algorithm-based driving condition observer model is built to observe the sideslip angle. The control accuracy of the vehicle stability control system is improved and the cost of vehicle condition observation is reduced.

In response to the problems of slow computation speed, complex learning process and susceptibility to local extremes in the late convergence of PSO-optimized FNN control in wheel motor-driven electric vehicle lateral stability control systems, the IPSO-FNN method for optimized control of wheel motor vehicle lateral sway stability is proposed. The lateral stability controller is also designed in a hierarchical control approach, with the upper layer being the lateral pendulum moment motion tracking layer and the lower layer being the moment optimisation distribution layer.

The results show that the overshoot of the mass side eccentricity control under the improved PSO-FNN is reduced

by 27%, while the convergence speed is increased by 2.5%, avoiding the problem that FNN control being prone to local extremes and improving the driving stability of wheel motor electric vehicles.

REFERENCES

[1] Z. P. Wang, X. L. Ding, L. Zhang, "Summary of key technologies for driving Anti-skid Control of four-wheel hub motor drive electric vehicle", *Journal of Mechanical Engineering*, vol. 55, no. 12, pp. 99–120, 2019.

[2] Z. H. Zhong, Y. J. Qiao, J. Q. Wang, et al. "Summary of strategy research on automobile power in a new era(1)", *Chinese Journal of Engineering Science*, vol. 20, no. 1, pp. 1–10, 2018.

[3] P. F. Yang, L. Xiong, et al. "Stability control strategy design and experiment of distributed electric drive vehicle", *Journal of Mechanical Engineering*, vol. 49, no. 24, pp. 128–134, 2013.

[4] L. F. Zhong, Y. H. Peng, M. Jiang, "Stability control of distributed driven electric vehicle based on phase plane", *Automotive Engineering*, vol. 43, no. 5, pp. 721–729+738, 2021.

[5] X. F. Yuan, Q. Y. Chen, G. M. Huang, et al. "Adaptive lateral stability control of electric vehicle based on FNN", *Journal of Hunan University (Natural Sciences)*, vol. 46, no. 8, pp. 98–104, 2019.

[6] G. Jun and A. J. Ma, "Research on optimal driver steering model based on multi-point preview", *Journal of Physics*: Conference Series, vol. 887, no. 1, pp. 012024–012024, 2017.

[7] C. WU, Y. LIU, "Queuing network modelling of driver workload and performance", *IEEE Transaction on Intelligent Transportation Systems*, vol. 8, no. 3, pp. 527–537, 2007.

[8] H. B. Zhou, Y. Zhang, X. Y. Bai, et al. "Model predictive control of nonlinear system based on the adaptive fuzzy neural network", *CIESC Journal*, vol. 71, no. 7, pp. 3201–3212, 2020.

[9] P. Hui and F. Liu and Z. R. Xu, "Variable universe fuzzy control for vehicle semi-active suspension system with MR damper combining fuzzy neural network and particle swarm optimization", Neurocomputing, vol. 306, pp. 130–140, 2018.

[10] S. A. Mirjalili and S. Z. M. Hashim and H. M. Sardroudi, "Training feedforward neural networks using hybrid particle swarm optimization and gravitational search algorithm", *Applied Mathematics and Computation*, vol. 218, no. 22, pp.11125–11137, 2012.

[11] W. Z. Sun, M. Zhang, J. S. Wang, S. S. Guo, M. Wang, and W. Kuo. Hao, "Binary Particle Swarm Optimization Algorithm Based on Z-shaped Probability Transfer Function to Solve 0-1 Knapsack Problem," *IAENG International Journal of Computer Science*, vol. 48, no.2, pp294–303, 2021

[12] Yi. X. Lu, J. S. Wang, and S. S. Guo, "Solving Path Planning Problem Based on Particle Swarm Optimization Algorithm with Improved Inertia Weights," *IAENG International Journal of Computer Science*, vol. 46, no.4, pp628–636, 2019

[13] R. L. Zhang et al. "Parametrical optimisation of particle dampers based on particle swarm algorithm", *Applied Acoustics*, vol. 160, no. C, pp. 107083–107083m, 2020.

[14] B. M. Wang, Z. G. Qi, et al. "Parameter identification of SCARA Robot based on random weight Particle Swarm Optimization", *Journal of Xi'an Jiaotong University*, vol. 55, no. 09, pp. 20–27, 2021.

[15] Y. X. Xing, J. S. Wang, Y. Zheng, and Y. C. Wang, "Particle Swarm Optimization Algorithm Based on Different Inertia Weights for Solving the P-Hub Allocation Problem," *IAENG International Journal of Applied Mathematics*, vol. 52, no.4, pp1025–1039, 2022.

[16] W. Hu, Z. S. Li, "A simpler and more effective Particle Swarm Optimization algorithm", *Journal of Software*, vol. 18, no. 4, pp. 861–868, 2007.

[17] X. Y. Cao, et al. "A research of simplified Particle Swarm Optimization algorithm with weight and learning factor", *International Core Journal of Engineering*, vol. 5, no. 12, pp. 85–92, 2019.

[18] Z. G. Z, Z. W. Zhang, et al. "Adaptive extended Particle Swarm Optimization algorithm", *Computer Engineering and Applications*, vol. 47, no. 18, pp. 45–47, 2011.

[19] D. Z. Li and W. L, "Wang and Ismail Fathy. Fuzzy neural network technique for system state forecasting", *IEEE Transactions on Cybernetics*, vol. 43, no. 5, pp. 1484–94, 2013.

[20] R. Rohit et al. "Design of optimal UKF State Observer-controller for stochastic dynamical systems", *IEEE Transactions on Industry Applications*, vol. 57, no. 2, pp. 1840–1859, 2021.

Zhigang Zhou is an associate professor of Henan University of Science and Technology. His research interests include the dynamics and control of new energy vehicles, dynamics, and dynamic reliability of mechanical transmission systems.